Loss of knee extensor torque complexity during fatiguing isometric muscle contractions occurs exclusively above the critical torque

Jamie Pethick, Samantha L. Winter and Mark Burnley

Endurance Research Group, School of Sport and Exercise Sciences, University of Kent, UK.

Running head: Loss of complexity above but not below the critical torque

Address for correspondence:
Dr Mark Burnley
School of Sport and Exercise Sciences
University of Kent
The Medway Building
Chatham Maritime
Kent
ME4 4AG
United Kingdom
m.burnley@kent.ac.uk

Abstract

The complexity of knee extensor torque time series decreases during fatiguing isometric muscle contractions. We hypothesised that, due to peripheral fatigue, this loss of torque complexity would occur exclusively during contractions above the critical torque (CT). Nine healthy participants performed isometric knee extension exercise (6 s contraction, 4 s rest) on 6 occasions for 30 min or to task failure, whichever occurred sooner. Four trials were performed above CT (trials S1-S4, S1 being the lowest intensity), and two were performed below CT (at 50% and 90% of CT). Global, central and peripheral fatigue were quantified using maximal voluntary contractions (MVCs) with femoral nerve stimulation. The complexity of torque output was determined using approximate entropy (ApEn) and the Detrended Fluctuation Analysis α scaling exponent (DFA α). The MVC torque was reduced in trials below CT (by [Mean ± SEM] 19 ± 4% in 90%CT), but complexity did not decrease (ApEn for 90%CT: from 0.82 ± 0.03 to 0.75 ± 0.06, 95% paired-samples confidence intervals, 95% CI = –0.23, 0.10; DFA α from 1.36 ± 0.01 to 1.32 ± 0.03, 95% CI –0.12, 0.04). Above CT, substantial reductions in MVC torque occurred (of 49 ± 8% in S1), and torque complexity was reduced (ApEn for S1: from 0.67 ± 0.06 to 0.14 ± 0.01, 95% CI = –0.72, –0.33; DFA α from 1.38 ± 0.03 to 1.58 ± 0.01, 95% CI 0.12, 0.29). Thus, in these experiments, the fatigue-induced loss of torque complexity occurred exclusively during contractions performed above the CT.

Keywords: non-linear dynamics; fractal scaling; exercise; central and peripheral fatigue

Introduction

Physiological systems produce outputs that inherently fluctuate when measured over time. These fluctuations in physiological time series, such as the force or torque output from a contracting muscle group, can be described in terms of their *magnitude*, using the standard deviation (SD) or the coefficient of variation (CV; 19, 28, 57). Alternatively, such fluctuations can be quantified according to their temporal *structure* or "complexity". In this context, a complex signal has a number of characteristic properties that the SD and/or spectral analysis cannot quantify, namely, temporal irregularity, time irreversibility, and long-range (fractal) correlations (21, 32, 44). No single statistic captures all of these properties. As a result, multiple analyses are required to determine the complexity of a physiological time series (22). Measures of complexity include those drawn from information theory, which quantify the regularity of fluctuations in a time series (such as approximate entropy, ApEn; 43, 44), and those drawn from fractal geometry, which quantify the long-range correlations present in a signal (such as detrended fluctuation analysis, DFA; 39). The DFA scaling exponent, α, differentiates signals possessing white ($\alpha \sim 0.5$), pink ($\alpha \sim 1.0$), or Brownian ($\alpha \sim 1.5$) noise. Using this analysis, pink noise is considered the most complex because it indicates the presence of self-similar fluctuations across multiple time scales (21). Complexity is thought to be a hallmark of healthy physiological systems (40). In the case of the neuromuscular system, the complexity of force or torque output is thought to reflect the ability to adapt motor output rapidly and accurately in response to alterations in demand (31, 59).

It has been proposed that the aging process and various disease states are characterized by a loss of physiological complexity (32). This "loss of complexity hypothesis" initially focused on heart rate dynamics (32), but it has also been shown to apply, *inter*

alia, to respiratory frequency (41), stride timing in normal walking (24) and, crucially, muscle force output (52, 56, 59). In the latter case, older adults produce less complex force output during a sustained finger abduction task than young subjects, suggesting that for the same relative force output motor control is diminished in older muscle (59). We have recently extended the loss of complexity hypothesis to acute neuromuscular system changes caused by fatigue in healthy young adults (42). In that study, repeated maximal and submaximal isometric contractions of the knee extensors resulted in the development of neuromuscular fatigue of both central and peripheral origin (i.e., fatigue residing in the central nervous system or the muscle, respectively), assessed using maximal voluntary contractions (MVCs) and supramaximal stimulation of the femoral nerve (42; for review see 20). The development of fatigue was accompanied by a loss of torque output complexity, measured by a progressive decrease in ApEn and a progressive increase in the DFA α exponent. The mechanism producing this loss of complexity is unclear, but it is well known that the mechanisms of fatigue are exercise intensity dependent (45). Specifically, the mechanism responsible for peripheral fatigue, as well as its rate of development, changes considerably as contractile intensity is increased above the so-called critical torque (CT; 8). It is likely that the submaximal contractions in our previous study (at 40% MVC) were performed above the CT, since CT has been shown to occur at ~25-35% MVC using the same contraction duty cycle (7, 8). Performing muscle contractions at a range of intensities straddling the CT should, therefore, provide crucial insights into the fatigue-induced loss of torque complexity.

The CT, analogous to the critical power frequently measured during dynamic whole-body exercise such as cycling (35; for reviews, see 30, 34), represents the asymptote of the hyperbolic relationship between torque output and time to task failure or "exhaustion" (7, 8). Dynamic exercise performed above the critical power is associated

with non-steady state profiles of pulmonary O_2 uptake ($\dot{V}O_2$; 46, 47) and muscle metabolism (29, 60), in contrast to the steady state profiles attainable below the critical power. Similarly, below CT the neuromuscular adjustments during intermittent contractions are modest (chiefly increased motor unit recruitment and/or firing frequency [1, 2], reflected indirectly in the amplitude of the electromyogram [EMG]), and the progression of fatigue is much slower than that during contractions performed above CT (8). Above CT, there is a progressive loss of MVC torque until task failure occurs, and at task failure the magnitude of peripheral fatigue is similar regardless of the duration of the task (7, 8). As such, the CT represents a critical metabolic (29) and neuromuscular fatigue threshold (8), and consequently metabolite-mediated peripheral fatigue is thought to be the dominant mechanism of torque losses above CT (7, 8). If the fatigue-induced loss of torque complexity (42) is mechanistically coupled to this form of peripheral fatigue, then such a loss should only occur during contractions performed above the CT. Furthermore, if the loss of complexity is related to the magnitude of peripheral fatigue development above CT (rather than simply task duration), then torque complexity should decrease to reach similar values at task failure, regardless of the duration of exercise producing that failure.

The purpose of the present study was to investigate the effect of fatigue on the complexity of knee extensor torque output in relation to the CT. To that end, we aimed to determine if different temporal profiles of knee extensor torque complexity are evident above and below the CT. The experimental hypothesis tested was that above the CT, central and peripheral fatigue would be evident and torque complexity would be progressively reduced, quantified by a decrease in ApEn and an increase in the DFA α exponent, whereas below CT fatigue would develop but torque complexity would not decrease.

Materials and Methods

Participants

Nine healthy participants (5 male, 4 female; mean ± SD: age 25.3 ± 5.8 years; height 1.74 ± 0.10 m; body mass 69.2 ± 10.4 kg) provided written informed consent to participate in the study, which was approved by the ethics committee of the University of Kent, and which adhered to the Declaration of Helsinki. Participants were instructed to arrive at the laboratory rested (having performed no heavy exercise in the preceding 24 hours) and not to have consumed any food or caffeinated beverages in the three hours before arrival. Participants attended the laboratory at the same time of day (± 2 hours) during each visit.

Experimental design

Participants were required to visit the laboratory on seven occasions over a four to six week period, with a minimum of 48 hours between visits. During their first visit, participants were familiarized with all testing equipment and procedures, and the settings for the dynamometer and stimulator were recorded. During visits two to five, participants performed a series of intermittent isometric contractions to task failure ("*severe trials*"; see below). From these four tests, the CT was calculated, and participants subsequently performed two further tests, during visits six and seven, at 50% and 90% of the torque at CT (50%CT and 90%CT respectively; "*sub-CT trials*"; see below) for 30 minutes or until task failure, whichever occurred first. The severe trials and the sub-CT trials were each presented in a randomized order. In each trial, torque output was sampled continuously to allow the quantification of complexity, muscle activity was measured using the *m. vastus lateralis* electromyogram (EMG), and MVCs with supramaximal femoral nerve stimulation performed before and immediately

after each trial were used to quantify global, central and peripheral fatigue, as detailed below.

Protocol

Electromyography and femoral nerve stimulation

During all visits on arrival at the laboratory participants had their right leg shaved and cleaned using an alcohol swab over the belly of the *vastus lateralis* and on the medial aspect of the proximal tibia. For EMG acquisition, two Ag/AgCl electrodes (Nessler Medizintechnik, Innsbruck, Austria) were placed on the belly of the *vastus lateralis* in line with the muscle fibers, and a single electrode was placed on the medial aspect of the tibia at the level of the tibial tuberosity. Care was taken to ensure that these electrode locations were identical between sessions. For femoral nerve stimulation, the anode (100 mm × 50 mm; Phoenix Healthcare Products Ltd, Nottingham, UK) was placed on the lower portion of the right gluteus maximus lateral to the ischial tuberosity. Participants then sat in the chair of a Cybex isokinetic dynamometer (HUMAC Norm; CSMi, Stoughton, MA, USA), with the lever arm set so that the relative knee angle was held at 90°. The chair's position was recorded and replicated in subsequent trials. The position of the cathode was located using a motor point pen (Compex; DJO Global, Guildford, UK), and another Ag/AgCl electrode was placed on that point. The establishment of the appropriate stimulator current (200 μs pulse width) was then performed as described by Pethick *et al*. (42), wherein current was incrementally increased until knee extensor torque and the compound motor unit action potential (M-wave) response to single twitches had plateaued and was verified during stimulation delivered during a contraction at 50% MVC to ensure a maximal M-wave during was also evident during an isometric contraction. The stimulator current was then increased

to 130% of the current producing a maximal M-wave. In all trials, doublet stimulation (two 200 μs pulses with 10 ms interpulse interval) was used.

All visits followed a similar pattern of data acquisition, beginning with the instrumentation of the participants and the (re-)establishment of the correct dynamometer seating position and supramaximal stimulation response. Participants then performed a series of brief (3 s) MVCs to establish their maximum torque. These contractions were separated by 60 s rest, and continued until three consecutive peak torques were within 5% of each other. Participants were given a countdown, followed by very strong verbal encouragement to maximize torque. The first MVC was used to establish the fresh maximal EMG signal, against which the subsequent EMG signals were normalized (*Data analysis*; see below). The second and third MVCs were performed with peripheral nerve stimulation. In all instances, where MVCs were performed with stimuli, the stimuli were manually delivered ~1.5 s into the contraction to coincide with maximal torque, and 2 s after the contraction to provide a resting potentiated doublet. Following the establishment of maximal torque, participants rested for 10 min, and then performed either one of the severe or sub-CT trials (see below). In all of these trials, at task end/failure participants immediately performed an MVC, which was accompanied by peripheral nerve stimulation.

Severe trials (performed above CT)

During visit two (the first of the severe trials), the highest instantaneous pre-test measure of voluntary torque was recorded as the peak MVC torque, and the target torques for the submaximal contractions in visits two to five were calculated from this value. The submaximal contractions were performed using a duty cycle of 0.6, with contractions held for 6 s, followed by 4 s rest. The target for the submaximal contractions in visit two was set at 50% of the peak torque measured in the pre-test

MVCs. Participants were instructed to match their instantaneous torque with a target bar superimposed on the display in front of them and were required to continue matching this torque for as much of the 6 s contraction as possible. The test was conducted until task failure, the point at which the participant failed to reach the target torque on three consecutive occasions, despite strong verbal encouragement. Participants were not informed of the elapsed time during the test, but were informed of each "missed" contraction. After the third missed contraction, participants were instructed to immediately produce an MVC, which was accompanied by peripheral nerve stimulation.

The duration of the initial severe trial at 50% MVC was used to determine the percentage of MVC used in subsequent trials, which were performed in an identical manner. The objective of these tests was to yield trial durations of between two and fifteen minutes, which have been recommended for the assessment of CT (25). The subsequent severe-intensity trials were performed in a randomized order. Visits two to five were used to determine the CT; individual trials were identified as severe 1 (S1) to severe 4 (S4), with S1 being the lowest and S4 being the highest torque.

Sub-CT trials

The final two visits were performed at target torques of 50% and 90% of the calculated CT (identified as 50%CT and 90%CT), the order of which was determined by a coin toss. These trials were conducted in the same manner as the severe trials, requiring the participants to perform intermittent contractions (6 s on, 4 s off) at a target torque. In these trials, the contractions continued for 30 min or until task failure, whichever occurred sooner. Immediately after completion of the trial or task failure, participants were instructed to perform an MVC, which was accompanied by peripheral nerve stimulation. The two sub-CT trials were performed in a randomized order.

Data acquisition and participant interface

Data acquisition was performed in the same manner as described in Pethick *et al*. (42). Briefly, all peripheral devices were connected via BNC cables to a Biopac MP150 (Biopac Systems Inc., California, USA) and a CED Micro 1401-3 (Cambridge Electronic Design, Cambridge, UK) interfaced with a personal computer. All signals were sampled at 1 kHz. The data were collected in Spike2 (Version 7; Cambridge Electronic Design, Cambridge, UK). A chart containing the instantaneous torque was projected onto a screen placed ~1 m in front of the participant. A scale consisting of a thin line (1 mm thick) was superimposed on the torque chart and acted as a target, so that participants were able to match their instantaneous torque output to the target torque during each test.

Data analysis

All data were processed and analyzed using code written in MATLAB R2013a (The MathWorks, Massachusetts, USA).

Torque and EMG. The mean and peak torque for each contraction in every test was determined. The mean torque was calculated based on the steadiest five seconds of each contraction. The torque impulse (the integral of torque and time) was also calculated for each contraction. The EMG signal from the *vastus lateralis* was filtered (10-500 Hz) full-wave rectified with a gain of 1000. The average rectified EMG (arEMG) for each contraction was then calculated and normalized by expressing the arEMG as a fraction of the arEMG obtained during an MVC from the fresh muscle performed at the beginning of each trial.

To determine task failure, the mean contraction torque produced in the first minute of the contractions was calculated, and task failure was deemed to have occurred when participants' mean torque output failed to achieve that in the first minute by more than 5 N.m for three consecutive contractions, with the first of these contractions being the time at which task failure occurred. To determine the CT, the total torque impulse produced until task failure and the total contraction time during each individual trial were calculated. The torque impulse was then plotted against the contraction time, and the parameters of the torque-duration relationship were estimated using linear regression of the torque impulse vs. contraction time (7, 8):

$$\text{Torque impulse} = W' + CT \cdot t \quad [1]$$

where W' represents the curvature constant parameter and t is the time to task failure.

Central and peripheral fatigue. Measures of central and peripheral fatigue were calculated based on the stimuli delivered during and after pre-test and task failure MVCs. Global fatigue was assessed using the fall in the MVC torque, peripheral fatigue was evidenced by a fall in the peak potentiated doublet torque, and central fatigue by the decline in voluntary activation (VA; 5):

$$VA = 1 - (\text{superimposed doublet}/\text{potentiated doublet}) \times 100 \quad [2]$$

The time to peak torque and the half-relaxation time were also calculated from each resting potentiated doublet. The time to peak torque was measured as the time from the delivery of the stimulus to the highest torque response, and the half-relaxation time was measured as half the time from the peak torque to the recovery of baseline torque. In

289 one participant during the CT50% trial, the stimulator failed to deliver a doublet
290 stimulus and the doublet data from that test were not used in the analysis.
291
292 *Variability and complexity*. All measures of variability and complexity were calculated
293 using the steadiest five seconds of each contraction, identified as the 5 seconds
294 containing the lowest standard deviation (SD). The amount of variability in the torque
295 output of each contraction was measured using the SD, which provides a measure of the
296 absolute amount of variability in a time series and coefficient of variation (CV), which
297 provides a measure of the amount of variability in a time series normalized to the mean
298 of the time series. Force accuracy was quantified by calculating the root mean squared
299 error (RMS error) between the target torque and the instantaneous torque during the
300 steadiest 5 seconds of each contraction.
301
302 The temporal structure, or complexity, of torque output was then examined using
303 multiple time domain analyses. To determine the regularity of torque output, we
304 calculated ApEn (43), and to estimate the temporal fractal scaling of torque detrended
305 fluctuation analysis (DFA) was used (39). Sample entropy was also calculated (48), but
306 as shown in Pethick *et al*. (42) this measure did not differ from ApEn, and was not
307 included in the present analysis. As detailed in Pethick *et al*. (42), ApEn was calculated
308 with the template length, *m*, set at 2 and the tolerance, *r*, set at 10% of the standard
309 deviation of torque output, and DFA was calculated across time scales (57 boxes
310 ranging from 1250 to 4 data points).
311
312 *Statistics*
313 All data are presented as means ± SEM. Two-way ANOVAs with repeated measures
314 were used to test for differences between conditions and time points, and for a
315 condition*time interaction for torque, arEMG, potentiated doublet torque, voluntary

316 activation, variability and complexity. The variability and complexity measures were
317 analyzed using means from the first minute and the final minute before task end/failure.
318 The rates of change in all parameters were analyzed using one-way ANOVAs with
319 repeated measures. Main effects were considered significant when $P < 0.05$. When
320 main effects were observed, Bonferroni-adjusted 95% paired-samples confidence
321 intervals were then used to determine specific differences.
322
323

Results

Preliminary measures and the CT

The peak instantaneous MVC torque recorded during an MVC in visit two was 198.1 ± 17.2 N.m. This was used to set the target torques for the four tests performed above CT, which ranged from 78.7 ± 6.3 to 112.7 ± 9.0 N.m, or 40.8 ± 2.6 to 57.8 ± 2.5% MVC (Table 1). The CT was calculated to be 57.5 ± 4.7 N.m, which was equivalent to 29.7 ± 1.7% MVC, and the W′ was 3637 ± 537 N.m.s. The 95% CI for the estimation of CT was 11.8 ± 2.3 N.m. The two trials below CT (50%CT and 90%CT) were performed at 28.7 ± 2.3 and 51.7 ± 4.2 N.m, or 14.9 ± 0.9 and 26.7 ± 1.6% MVC, respectively (Table 1).

Torque and EMG

For the trials above the CT, task failure occurred when participants were no longer able to achieve the target torque, despite a maximal effort. All trials above the CT resulted in significant decreases in MVC torque ($F = 62.17$, $P < 0.001$), with the mean MVC torque at task failure being not significantly different from (S1-S3) or significantly lower than (S4) the torque produced during the submaximal contractions (Table 1). In contrast, all participants completed 30 minutes of contractions in both trials below the CT. At the end of these trials, the mean MVC torque was still significantly greater than the submaximal torque requirements (paired-samples confidence intervals (CIs): 90%CT, 52.6, 168.2 N.m; 50%CT, 92.2, 211.3 N.m), indicating that contractions performed below the CT ended with a substantial reserve in maximal torque.

The arEMG amplitude increased over time in all of the trials above the CT, reaching ~61-77% of the pre-test MVC value at task failure ($F = 14.33$, $P = 0.005$; Table 1). Contractions below the CT resulted in only modest increases in arEMG as the trials

progressed, with the values at task end not significantly different from those at the start (CIs: 90%CT, –4.7, 19.0%; 50%CT, –0.6, 2.9%).

Peripheral and central fatigue

All the trials above the CT resulted in significant reductions in potentiated doublet torque ($F = 34.34$, $P = 0.001$; Table 1), indicating the presence of peripheral fatigue. The potentiated doublet torque attained at task failure was not significantly different between trials above CT (CIs: S1 vs. S2 –19.2, 20.5 N.m; S1 vs. S3, –10.9, 12.4 N.m; S1 vs. S4, –11.9, 17.2 N.m; Table 1). The time to peak tension ($F = 2.85$, $P = 0.15$) and half-relaxation time ($F = 0.34$, $P = 0.62$) were unaffected by contractions above CT. Voluntary activation significantly declined during all trials above the CT ($F = 192.21$, $P < 0.001$; Table 1), indicating the presence of central fatigue. The potentiated doublet torque was reduced in both trials below CT, but not to the same extent as trials above CT (Table 1). Voluntary activation also significantly decreased in 90%CT (CI: –9.4, –1.7%). There was no change in voluntary activation during contractions at 50%CT (CI: –5.9, 3.5%).

Variability and complexity

The variability and complexity data are presented in Table 2. All trials above the CT resulted in a significant increase in the amount of variability, as measured by the SD ($F = 110.15$, $P < 0.001$) and CV ($F = 136.96$, $P < 0.001$). The values attained at task failure for the SD were not significantly different across trials above CT. The trials below the CT resulted in no change in the amount of variability (SD CIs: 90%CT,–0.1, 0.7 N.m; 50%CT, –0.1, 0.5 N.m; CV: 90%CT, –0.2, 1.5%; CT50%, –0.1, 2.0%), and the values at task end were significantly lower than those at task failure in the trials above the CT (Table 2). Force accuracy was higher in the CT50% and CT90% trials than in S1 ($F =$

23.06, P <0.001), and accuracy declined only during contractions performed above the CT (F = 101.5, P < 0.001, Table 2).

Complexity at the beginning of the trials decreased with increasing torque requirements from 50%CT to S4 (ApEn, F = 35.54, P < 0.001; DFA α, F = 38.97, P < 0.001; Figure 1). Representative time series of torque output during contractions below and above CT are shown in Figure 2. All trials above the CT resulted in decreases in complexity, as measured by ApEn (F = 192.30, P < 0.001) and DFA α (F = 46.28, P < 0.001; Figure 2; Figure 3). ApEn decreased as the trials progressed, with the values at task failure in S1-S4 being similar, despite different starting values (Table 2; Figure 1A). DFA α increased, indicating more Brownian-like noise, as the trials progressed, with no significant differences between trials for the values at task failure. In contrast, the trials below the CT resulted in no significant change in complexity after 30 min of contractions: ApEn CIs, 90%CT, –0.23, 0.10; 50%CT, –0.29, 0.05; DFA α CIs 90%CT, –0.12, 0.04; 50%CT, –0.06, 0.11. At the end of these tasks the values were significantly higher (ApEn) or lower (DFA α) than at task failure above CT (Table 2; Figure 1B; Figure 3).

Rates of fatigue development

The rates of decrease in MVC torque, potentiated doublet torque and voluntary activation all increased with increasing torque requirements from 50%CT to S4 and were significantly greater above compared to below the CT (MVC, F = 34.41, P < 0.001; potentiated doublet, F = 16.68, P = 0.002; voluntary activation, F = 17.71, P = 0.001; Table 1). The rate of increase in arEMG also increased with increasing torque requirements and was significantly greater above compared to below the CT (F = 8.63, P = 0.008; Table 1).

The rate of decrease in ApEn (Figure 4A) increased with increasing torque requirements from 90%CT to S4 and was significantly greater above compared to below the CT (ApEn, $F = 34.94$, $P < 0.001$; Table 2). The rate of increase in DFA α (Figure 4B) increased with increasing torque requirements from 90%CT to S4 and was significantly greater above compared to below the CT ($F = 14.52$, $P = 0.001$; Table 2).

Discussion

The major novel finding of this investigation was that the complexity of knee extensor torque output was reduced during contractions performed exclusively above the critical torque. Contractions performed above CT were associated with the development of substantial central and peripheral fatigue, accompanied by reduced complexity and increasingly Brownian (DFA α = 1.50) fluctuations in torque output. At task failure above CT, torque complexity, voluntary activation and the potentiated doublet torque all fell to reach similar values regardless of the torque requirement of the task. In contrast, contractions below the CT resulted in no change in the complexity of torque output, in spite of the development of peripheral fatigue (at 50% and 90%CT) and central fatigue (at 90%CT). These results provide new evidence that torque complexity is sensitive to the development of neuromuscular fatigue only during high-intensity (>CT) voluntary contractions.

Effect of fatigue on the magnitude of torque fluctuations: variability vs. complexity

The contractions performed above the CT led to a marked increase in the SD, CV and RMS error of torque fluctuations, whereas contractions below the CT did not (Table 2). A fatigue-induced increase in the amplitude of torque fluctuations during isometric contractions has been repeatedly observed (10, 18, 26). Whilst a progressive increase in the amplitude of torque fluctuations mirrors the loss of torque output complexity, it is

431 important to appreciate that measures of complexity quantify different properties of the
432 torque signal (31). Specifically, the ApEn statistic quantifies regularity by identifying
433 template matches in a time series, with fewer matches indicating greater complexity,
434 and the DFA α exponent identifies noise color and, if present, long-range correlations.
435 The DFA α exponent increasing above unity towards ~1.5 (as seen the present study)
436 also indicates a less complex, Brownian noise-like signal. Crucially, changes in time
437 series complexity can be observed in the absence of changes in the magnitude of
438 fluctuations (i.e., the SD), as reported, for example, in postural tremor in Parkinson's
439 patients (58). Thus, the temporal structure of physiological time series contains
440 information additional to, and distinct from, amplitude-based measures of time series
441 variability (32).
442
443 *Neuromuscular fatigue and complexity below and above the critical torque*
444 The fatigue-induced loss of torque complexity we previously reported was observed
445 during either a series of MVCs or contractions performed at 40% MVC to task failure
446 (42). By utilizing a broad range of target torques in the present study (from ~15-60%
447 MVC), we aimed to examine whether the fatigue-induced loss of complexity was
448 dependent on contractile intensity, with specific reference to the CT. Although the
449 critical power (or torque) was originally proposed to represent a power (or torque)
450 below which fatigue would not occur (34), it is now known that fatigue does develop
451 below the CT, but at a disproportionately slower rate than above CT (8). The results of
452 the present study support this, with the decrease in MVC torque occurring more than
453 four times faster for the S1 trial compared to the 90%CT trial, and with the rate of
454 fatigue in all its forms increasing as the torque demands increased above CT (Table 1).
455 It is thought that the dominant mechanism of fatigue above CT is metabolite-induced
456 peripheral fatigue (7, 8), on the basis that progressive phosphorylcreatine (PCr)
457 depletion and phosphate (P_i) and H^+ accumulation only occur above the CT (29, 60). P_i

458 accumulation, in particular, has been associated with fatigue in skinned fiber
459 preparations (15, 37), either through a direct effect on crossbridge force (12, 38), or
460 through depressive effects on Ca^{2+} kinetics (15). Recently, it has also been suggested
461 that the effects of P_i and H^+ accumulation are additive (36), resulting in profound
462 peripheral fatigue during high-force contractions. The loss of muscle force-generating
463 capacity *in vivo* results in additional motor unit recruitment to sustain the demands of
464 the task (1, 2), reflected, albeit indirectly, by an increase in *vastus lateralis* EMG
465 amplitude (Table 1). Collectively, these metabolic and neuromuscular responses drive
466 the non-steady state increases in muscle and pulmonary $\dot{V}O_2$ that occur above the
467 critical power/torque (46, 49, 61). As a result, neuromuscular fatigue above critical
468 power leads to a progressive decrease in muscular efficiency (23).
469
470 The present investigation adds a further dimension to the critical power concept,
471 because for the first time we show that the fatigue-induced loss of torque output
472 complexity we previously reported (42) occurs only above the CT. Specifically, above
473 the CT the ApEn statistic decreased (indicating increased signal regularity) and the DFA
474 α exponent increased towards values approximating Brownian noise (~1.5, Table 2,
475 Figures 2 and 3). Both metrics indicate a progressive reduction in the complexity of the
476 torque signal as fatigue develops above, but not below, CT. The factors that link this
477 loss of complexity with CT are not clear, but Seely and Macklem (50) have
478 hypothesized a link between a system's prevailing metabolic rate and its output
479 complexity. Our results support this hypothesis, since it is only above the CP/CT that
480 muscle $\dot{V}O_2$ rises inexorably as a function of time, and we show here that complexity
481 only falls as a function of time above CT. Thus, it is possible that the loss of
482 complexity observed in the present study is linked to the distinct metabolic,
483 neuromuscular and respiratory perturbations that occur above the critical power/torque.
484

Despite the lack of change in complexity during contractions below the CT, a modest degree of global, central and peripheral fatigue was nevertheless observed in these conditions (Table 1). Specifically, by the end of the task in both the 50%CT and 90%CT trials, the potentiated doublet torque had declined, and at 90%CT the voluntary activation had decreased. This suggests that complexity is dissociated from the development of central and peripheral fatigue below the CT, and that fatigue mechanisms particular to contractions above CT are responsible for the loss of complexity we observed. Below CT, the responses of PCr, P_i and pH to exercise (29) are probably too small to affect the neuromuscular system's submaximal output to any significant degree. Thus, the neuromuscular system's freedom to explore and achieve control solutions (i.e., its "adaptability", reflected by its output complexity; 31, 40, 51, 59) is not significantly perturbed and contractions continue with relative ease. These results considerably advance our previous findings on both neuromuscular fatigue (8) and torque complexity (42) in that they demonstrate that metrics derived from the field of non-linear dynamics can be used to identify changes in neuromuscular system behavior coincident with the CT.

Physiological bases for changes in torque complexity above critical torque

During fatiguing submaximal contractions, the neuromuscular system must maintain the torque output in the face of reduced muscle fiber twitch forces (3) and motoneurone excitability (33), by increasing central drive and thus motor unit recruitment and rate coding (1, 6, 14). As the fatiguing contractions progress, therefore, a greater pool of fibers is engaged in the task, but due to peripheral fatigue each fiber contributes progressively less to the torque output. The net effect of this would likely be a smoothing of the torque time series, and thus reduced torque complexity (Figures 2 and 3; 42). Although we observed no change in the time to peak tension or the half-relaxation time in response to doublet stimulation of the femoral nerve (Table 1), a

512 slowing of these responses has been reported previously (9, 27) and could, if present,
513 also contribute to a smoothing of the torque time series. That the fatigue-induced loss
514 of complexity appears to occur exclusively above the CT (at least for tasks lasting 30
515 min or less) is crucial, because it suggests that only metabolite-mediated peripheral
516 fatigue is capable of commencing the chain of events leading to the loss of torque
517 complexity. These events seem to include both peripheral alterations and the central
518 adjustments required to counter them in order to continue exercise.
519
520 One of the central adjustments that may be key to the fatigue-induced loss of
521 complexity is the common synaptic input to motoneurons and the modulation of motor
522 unit discharge rates (i.e., common drive; 13, 16). A necessary consequence of a
523 common synaptic input to all motoneurons is the correlated discharge of action
524 potentials, known as motor unit synchronization (16). It has recently been demonstrated
525 that there is an increase in common synaptic input when the net excitatory input to
526 motoneurons increases, whether this is due to an increase in contraction intensity or to
527 the progression of fatigue and the necessary recruitment of a greater proportion of the
528 motor unit pool (11). The fatiguing contractions performed in Castronovo *et al*. (20-
529 75% MVC; 11) were likely to have been above the "critical force" for the tibialis
530 anterior, since critical force typically occurs at ~15% MVC for sustained contractions
531 (34). The present study demonstrates that both increased contractile intensity and
532 neuromuscular fatigue are also associated with decreased torque output complexity
533 (Figure 1, Table 2). Consequently, if common synaptic input explains most of the
534 variance in torque fluctuations (16, 17), then our results imply that fatigue processes
535 may influence the temporal complexity of common synaptic input and thus neural drive
536 to the muscle (17). However, the EMG measurements made in the present study (using
537 a single set of bipolar surface electrodes) did not allow us to address this hypothesis.
538 Nevertheless, common synaptic input oscillating at a single dominant frequency has

been suggested to cause the increased regularity of loaded postural tremor with aging (55).

As we have previously observed (8), peripheral fatigue developed more than four times faster above than below CT, and its rate of development accelerated as the torque requirements increased above CT (Figure 4B; Table 1). At task failure, however, the potentiated doublet had declined to similar levels, regardless of its rate of change or the intensity of the contractions themselves (Table 1). This is consistent with previous data demonstrating a consistent level of metabolic disturbance and/or peripheral fatigue at task failure (4, 8, 60). A major novel finding of the present investigation was that at task failure the values of ApEn and DFA α were similar for each of the trials above the CT, regardless of their starting values and their rate of change during the trials (Table 2). This indicates that task failure is characterized not only by consistent levels of metabolic disturbance and peripheral fatigue, but also by consistently low levels of torque complexity (Figure 1). Whether low complexity torque output plays a direct role in precipitating task failure is not presently clear (42). Nevertheless, a high level of physiological complexity is thought to be advantageous because it endows physiological systems with the ability to rapidly adapt to sudden changes in demand (31, 32, 40, 54). A loss of motor output complexity is associated with diminished motor control in aging (53-55, 59). In the present study, the high-frequency fluctuations present at the beginning of the trials above CT were progressively attenuated as task failure approached, giving way to large, low-frequency fluctuations (Figure 2B). These patterns are a signature of the neuromuscular system becoming unable to consistently match the target demand (54). At task failure, torque complexity reached consistently low values that may have compromised motor control and therefore limited task performance, in agreement with the purported functional importance of physiological complexity (31, 40, 54, 59). Thus, a role for low torque complexity in the mechanism

of task failure is plausible, but further studies are required to directly test this hypothesis.

Perspectives and Significance

The loss of torque complexity that occurred during fatiguing contractions above the CT in this study extends the "loss of complexity hypothesis" developed in aging and disease (32) to high-intensity (>CT) contractions in young healthy participants. Exploration of the central and peripheral mechanisms of this loss of torque complexity should, therefore, center on muscle contractions performed above the CT. The loss of complexity observed above CT implies that adaptability of the neuromuscular system is progressively compromised, which likely contributes to the processes resulting in task failure. Whether the fatigue-induced loss of complexity occurs when the target torque is varied (during sinusoidal or ramp-and-hold contractions, for example; 1, 59), or when dynamic contractions are performed in tasks such as cycling, is not clear. Establishing the effect of fatigue on neuromuscular output complexity in a range of tasks, and establishing the central and peripheral processes involved are, therefore, important next steps. Given the development of wearable or equipment-mounted devices to measure neuromuscular output during exercise, such work could pave the way to real-time assessment of the fatigue process in free running conditions.

Disclosures:

This work was supported by a University of Kent 50th Anniversary Scholarship. No external funding was received for this work. The authors report no conflicts of interest, financial or otherwise.

593 **Figure legends**

594

595 **Figure 1**

596 **Relationship between knee extensor torque requirement and torque complexity**

597 Panel A shows the approximate entropy measured in the first minute and in the last
598 minute of each intermittent contraction trial. Panel B shows the DFA α scaling
599 exponent measured in the same trials as panel A. Each trial (50%CT, 90%CT, S1-S4) is
600 highlighted between the two panels. CT occurred at 29.7 ± 1.7% MVC. Note that
601 complexity is significantly decreased (as shown by reduced ApEn and increased DFA α
602 exponent) only during contractions above the CT (white triangles). All values are mean
603 ± SEM.

604

605 **Figure 2**

606 **Responses of knee extensor torque during representative contractions below and**
607 **above the critical torque**

608 Panel A shows three contractions from the 90%CT trial in a representative participant:
609 one in the first minute (3^{rd} contraction), one at the mid-point (90^{th} contraction), and one
610 at the end of the task (180^{th} contraction). Notice that there is no change in the measures
611 of torque complexity as contractions progress. The amplitude of fluctuations appear
612 greater at the mid-point and at the end of the task by virtue of a slightly larger SD in
613 these contractions (1.4, 1.8, and 1.9 N.m, in first minute, mid-point and task end,
614 respectively). In panel B, data are taken from a test performed at 50% MVC (S3 trial),
615 in which task failure occurred in 3 min 50 s. The first minute is represented by the 2^{nd}
616 contraction of the test, the mid-point by the 12^{th} contraction (2 min) and task failure by
617 the 22^{nd} contraction (immediately preceding task failure). Notice the progressive loss of
618 torque complexity in each contraction (shown by the decreased ApEn and increased
619 DFA α exponent).

Figure 3

Time course of complexity in response to contractions below and above the critical torque

Panel A shows approximate entropy (ApEn), Panel B shows the Detrended Fluctuation Analysis α scaling exponent ("DFA α exponent"). In each panel, the white circles represent the 90%CT trial (below CT) and the black circles the S1 trial (the lowest torque performed above CT). Note the progressive decrease in ApEn and the progressive increase in the DFA α exponent during contractions above the CT, with no change during contractions below the CT. All values are mean ± SEM.

Figure 4

Rate of change in torque complexity in relation to torque requirements

Panels A and B show the rate of change in ApEn and the DFA α exponent, respectively. White circles, trials below CT; black symbols, trials above CT. Note that the rates of change for all variables are different from zero only above CT, and these rates increase as torque requirements are increased above CT. All values are mean ± SEM.

References

1. **Adam A, De Luca CJ.** Recruitment order of motor units in human vastus lateralis muscle is maintained during fatiguing contractions. *J Neurophysiol* 90: 2919-2927, 2003.

2. **Adam A, De Luca CJ.** Firing rates of motor units in human vastus lateralis muscle during fatiguing isometric contractions. *J Appl Physiol* 99: 268-280, 2005.

3. **Allen DG, Lamb GD, Westerblad H.** Skeletal muscle fatigue: cellular mechanisms. *Physiol Rev* 88: 287-332, 2008.

4. **Amann M, Romer LM, Subudhi AW, Pegelow DF, Dempsey JA.** Severity of arterial hypoxaemia affects the relative contributions of peripheral muscle fatigue to exercise performance in humans. *J Physiol* 581: 389-403, 2007.

5. **Behm DG, St-Pierre DMM, Perez D.** Muscle inactivation: assessment of interpolated twitch technique. *J Appl Physiol* 81: 2267-2273, 1996.

6. **Bigland-Ritchie B, Furbush F, Woods JJ.** Fatigue of intermittent submaximal voluntary contractions: central and peripheral factors. *J Appl Physiol* 61: 421-429, 1986.

7. **Burnley M.** Estimation of critical torque using intermittent isometric maximal voluntary contractions of the quadriceps in humans. *J Appl Physiol* 106: 975-983, 2009.

8. **Burnley M, Vanhatalo A, Jones AM.** Distinct profiles of neuromuscular fatigue during muscle contractions below and above the critical torque in humans. *J Appl Physiol* 113: 215-223, 2012.

9. **Cady EB, Elshove H, Jones DA, Moll A.** The metabolic causes of slow relaxation in fatigued human skeletal muscle. *J Physiol* 418: 327-337, 1989.

10. **Contessa P, Adam A, De Luca CJ.** Motor unit control and force fluctuation during fatigue. *J Appl Physiol* 107: 235-243, 2009.

11. **Castronovo AM, Negro F, Conforto S, Farina D.** The proportion of synaptic input to motor neurons increases with an increase in net excitatory input. *J Appl Physiol* 119: 1337-1346, 2015.

12. **Debold EP, Romatowski J, Fitts RH.** The depressive effect of Pi on the force-pCa relationship in skinned single muscle fibers is temperature dependent. *Am J Physiol Cell Physiol* 290: C1041-50, 2006.

13. **De Luca CJ, Erim Z.** Common drive of motor units in regulation of muscle force. *Trends Neurosci*, 17: 299-305, 1994.

14. **Dideriksen JL, Enoka RM, Farina D.** Neuromuscular adjustments that constrain submaximal EMG amplitude at task failure of sustained isometric contractions. *J Appl Physiol* **111**, 485-494, 2011.

15. **Dutka TL, Cole L, Lamb GD.** Calcium phosphate precipitation in the sarcoplasmic reticulum reduces action potential-mediated Ca^{2+} release in mammalian skeletal muscle. *Am J Physiol Cell Physiol* 289: C1502-C1512, 2005.

16. **Farina D, Negro F.** Common synaptic input to motor neurons, motor unit synchronization and force control. *Exerc Sport Sci Rev* 43: 23-33, 2015.

17. **Farina D, Negro F, Dideriksen JL.** The effective neural drive to muscles is the common synaptic input to motor neurons. *J Physiol* 592: 3427-3441, 2014.

18. **Furness P, Jessop J, Lippold OCJ.** Long-lasting increases in the tremor in human hand muscles following brief, strong effort. *J Physiol* 265: 821-831, 1977.

19. **Galganski ME, Fuglevand AJ, Enoka RM.** Reduced control of motor output in a human hand muscle of elderly participants during submaximal contractions. *J Neurophysiol* 69: 2108-2115, 1993.

20. **Gandevia SC.** Spinal and supraspinal factors in human muscle fatigue. *Physiol Rev* 81: 1725-1789, 2001.

21. **Goldberger AL, Amaral LAN, Hausdorff JM, Ivanov PC, Peng CK, Stanley HE.** Fractal dynamics in physiology: Alterations with disease and aging. *Proc Nat Acad Sci* 99: 2466-2472, 2002.

22. **Goldberger AL, Peng C-K, Lipsitz LA.** What is physiologic complexity and how does it change with aging and disease? *Neurobiol Aging* 23: 23-26, 2002.

715 23: **Grassi B, Rossiter HB, Zoladz JA.** Skeletal muscle fatigue and decreased
716 efficiency: two sides of the same coin? *Exerc Sport Sci Rev* 43: 75-83, 2015.
717
718 24. **Hausdorff JM, Mitchell SL, Firtion R, Peng CK, Cudkowicz ME, Wei JY,**
719 **Goldberger AL.** Altered fractal dynamics of gait: reduced stride-interval correlations
720 with aging and Huntington's disease. *J Appl Physiol* 82: 262-269, 2001.
721
722 25. **Hill DW.** The critical power concept: A review. *Sports Med* 16: 237-254, 1993.
723
724 26. **Hunter SK, Enoka RM.** Changes in muscle activation can prolong the endurance
725 time of a submaximal isometric contraction in humans. *J Appl Physiol* 94: 108-118,
726 2003.
727
728 27. **Jones DA, Turner DL, McIntyre DB, Newham DJ.** Energy turnover in relation to
729 slowing of contractile properties during fatiguing contractions of the human anterior
730 tibialis muscle. *J Physiol* 587: 4329-4338, 2009.
731
732 28. **Jones KE, Hamilton AFDC, Wolpert DM.** Sources of signal-dependent noise
733 during isometric force production. *J Neurophysiol* 88: 1533-1544, 2002.
734
735 29. **Jones AM, Wilkerson DP, DiMenna F, Fulford J, Poole DC.** Muscle metabolic
736 responses to exercise above and below the "critical power" assessed using ^{31}P-MRS. *Am*
737 *J Physiol Regul Integr Comp Physiol* 294: R585-R593, 2008.
738
739 30. **Jones AM, Vanhatalo A, Burnley M, Morton RH, Poole DC.** Critical power:
740 implications for the determination of $\dot{V}O_2$ max and exercise tolerance. *Med Sci Sports*
741 *Exerc* 42: 1876-1890, 2010.

31. **Lipsitz LA.** Dynamics of stability: the physiologic basis of functional health and frailty. *J Gerontol A Biol Sci Med Sci* 57A: B115-B125, 2002.

32. **Lipsitz LA, Goldberger AL.** Loss of 'complexity' and aging: Potential applications of fractals and chaos theory to senescence. *JAMA* 267: 1806-1809, 1992.

33. **McNeil CJ, Giesebrecht S, Gandevia SC, Taylor JL.** Behaviour of the motoneurone pool in a fatiguing submaximal contraction. *J Physiol* 589: 3533-3544, 2011.

34**. Monod H, Scherrer J.** The work capacity of a synergic muscular group. *Ergonomics* 8: 329-338, 1965.

35. **Moritani T, Nagata A, deVries HA, Muro M.** Critical power as a measure of physical work capacity and anaerobic threshold. *Ergonomics* 24: 339-350, 1981.

36. **Nelson CR, Fitts RH.** Effects of low cell pH and elevated inorganic phosphate on the pCa-force relationship in single muscle fibers at near-physiological temperatures. *Am J Physiol Cell Physiol* 306: C670-C678, 2014.

37. **Nosek TM, Fender KY, Godt RE.** It is diprotonated inorganic phosphate that depresses force in skinned skeletal muscle fibers. *Science* 236: 191-193, 1987.

38. **Palmer S, Kentish JC.** The role of troponin C in modulating the Ca^{2+} sensitivity of mammalian skinned cardiac and skeletal muscle fibres. *J Physiol* 480: 45-60, 1994.

39. **Peng C-K, Buldyrev SV, Havlin S, Simon M, Stanley HE, Goldberger AL.** Mosaic organization of DNA nucleotides. *Phys Rev E* 49: 1685-1689, 1994.

40. **Peng C-K, Costa M, Goldberger AL.** Adaptive data analysis of complexity fluctuations in physiologic time series. *Adv Adapt Data Anal* 1: 61-70, 2009.

41. **Peng C-K, Mietus JE, Liu Y, Lee C, Hausdorff JM, Stanley HE, Goldberger AL & Lipsitz LA.** Quantifying fractal dynamics of human respiration: age and gender effects. *Ann Biomed Eng* 30: 683–692, 2002.

42. **Pethick J, Winter SL, Burnley M.** Fatigue reduces the complexity of knee extensor torque fluctuations during maximal and submaximal intermittent isometric contractions in man. *J Physiol* 593: 2085-2096, 2015.

43. **Pincus SM.** Approximate entropy as a measure of system complexity. *Proc Nat Acad Sci* 88: 2297-2301, 1991.

44. **Pincus SM.** Greater signal regularity may indicate increased system isolation. *Math Biosci* 122: 161-181, 1994.

45. **Place N, Bruton JD, Westerblad H.** Mechanisms of fatigue induced by isometric contractions in exercising humans and in mouse isolated single muscle fibres. *Clin Exp Pharmacol Physiol* 36: 334–339, 2009.

46. **Poole DC, Ward SA, Gardner GW, Whipp BJ.** Metabolic and respiratory profile of the upper limit for prolonged exercise in man. *Ergonomics* 31: 1265-1279, 1988.

796 47. **Poole DC, Ward SA, Whipp BJ.** The effects of training on the metabolic and
797 respiratory profile of high-intensity cycle ergometer exercise. *Eur J Appl Physiol* 59:
798 421-429, 1990.
799
800 48. **Richman JS, Moorman JR.** Physiological time-series analysis using approximate
801 and sample entropy. *Am J Physiol Heart Circ Physiol* 278, H2039-H2049, 2000.
802
803 49. **Saugen E, Vøllestad NK.** Metabolic heat production during fatigue from voluntary
804 repetitive isometric contractions in humans. *J Appl Physiol* 81: 1323-1330, 1996.
805
806 50. **Seely AJE, Macklem P.** Fractal variability: An emergent property of complex
807 dissipative systems. *Chaos* 22: 013108, 2012.
808
809 51. **Sejdić E, Lipsitz LA.** Necessity of noise in physiology and medicine. *Comput*
810 *Methods Programs Biomed* 111: 459-470, 2013.
811
812 52. **Slifkin AB, Newell KM.** Noise, information transmission, and force variability. *J*
813 *Exp Psych* 25: 837-851, 1999.
814
815 53. **Sosnoff JJ, Newell KE.** Age-related loss of adaptability to fast time scales in motor
816 variability. *J Gerontol* 63: 344-352, 2008.
817
818 54. **Sosnoff JJ, Vaillancourt DE, Newell KM.** Aging and rhythmical force output: loss
819 of adaptive control of multiple neural oscillators. *J Neurophysiol* 91: 172-181, 2004.
820
821 55. **Sturman MM, Vaillancourt DE, Corcos DM.** Effects of aging on the regularity of
822 physiological tremor. *J Neurophysiol*, 93: 3064-3074, 2005.

56. **Svendsen JH, Madeleine P.** Amount and structure of force variability during short, ramp and sustained contractions in males and females. *Hum Mov Sci* 29: 35-47, 2010.

57. **Taylor AM, Christou EA, Enoka RM.** Multiple features of motor-unit activity influences force fluctuations during isometric contractions. *J Neurophysiol* 90: 1350-1361, 2003.

58. **Vaillancourt DE, Newell KM.** The dynamics of resting and postural tremor in Parkinson's disease. *Clin Neurophysiol* 111: 2046-2056, 2000.

59. **Vaillancourt DE, Newell KM.** Ageing and the time and frequency structure of force output variability. *J Appl Physiol* 94: 903-912, 2003.

60. **Vanhatalo A, Fulford J, DiMenna F, Jones AM.** Influence of hyperoxia on muscle metabolic responses and the power-duration relationship during severe-intensity exercise in humans: a ^{31}P magnetic resonance spectroscopy study. *Exper Physiol* 95: 528-540, 2010.

61. **Vøllestad NK, Wesche J, Sejersted OM.** Gradual increase in leg oxygen uptake during repeated submaximal contractions in humans. *J Appl Physiol* 68: 1150-1156, 1990.

Table 1. Voluntary torque, peripheral and central fatigue parameters, and EMG responses to contractions below (50%CT and 90%CT) and above (S1-S4) the critical torque.

Parameter	50%CT	90%CT	S1	S2	S3	S4
Mean test torque, N.m	28.7 ± 2.3	51.7 ± 4.2	78.7 ± 6.3	89.7 ± 6.8	104.0 ± 8.4	112.7 ± 9.0
Mean test torque, [a] % MVC	14.9 ± 0.9	26.7 ± 1.6	40.8 ± 2.6	46.7 ± 3.2	53.9 ± 3.4	57.8 ± 2.5
Time to task end/failure, min	30.0 ± 0.0	30.0 ± 0.0	17.5 ± 1.3	8.1 ± 0.7	4.8 ± 0.5	2.9 ± 0.3
Global fatigue						
Pre-exercise MVC, N.m	226.2 ± 19.7	223.8 ± 21.8	199.9 ± 18.6	198.1 ± 17.2	200.6 ± 15.5	209.6 ± 19.2
Peak MVC at task end/failure, N.m	205.6 ± 18.6†‡	182.2 ± 19.5†‡	101.9 ± 8.2†	110.7 ± 9.7†	119.4 ± 10.2†	112.7 ± 8.0†
Mean MVC at task end/failure, N.m	180.5 ± 18.3*	162.1 ± 17.8*	77.7 ± 5.7	87.4 ± 8.1	101.0 ± 8.5	95.1 ± 7.6*
ΔMVC/Δt, N.m.min^{-1}	–0.7 ± 0.1‡	–1.4 ± 0.3‡	–6.2 ± 1.3	–12.2 ± 1.8‡	–18.5 ± 3.2‡	–36.4 ± 5.5‡
Peripheral fatigue						
Pre-exercise doublet, N.m	97.2 ± 7.3	98.6 ± 8.5	95.1 ± 7.9	94.4 ± 8.7	92.3 ± 8.5	91.9 ± 7.7
Doublet at task end/failure, N.m	90.8 ± 6.9†‡	86.3 ± 7.6†‡	63.5 ± 4.9†	63.8 ± 8.1†	62.8 ± 5.0†	60.9 ± 6.3†
% Change at task end/failure	6.6 ± 1.3	12.5 ± 2.3	32.2 ± 3.8	32.6 ± 4.9	29.8 ± 5.2	32.7 ± 5.5
Δdoublet/Δt, N.m.min^{-1}	–0.2 ± 0.05‡	–0.4 ± 0.1‡	–1.8 ± 0.4	–3.9 ± 0.7‡	–6.1 ± 1.3‡	–11.6 ± 2.5‡
Time to peak torque						
Pre-exercise, ms	91.3 ± 1.7	93.4 ± 2.4	95.4 ± 4.8	94.6 ± 4.5	94.9 ± 4.9	93.6 ± 2.8
At task end/failure, ms	92.1 ± 2.2	91.6 ± 2.5	86.8 ± 1.6	90.8 ± 3.2	91.9 ± 4.4	91.9 ± 2.2
One-half relaxation time						
Pre-exercise, ms	201.7 ± 31.7	162.3 ± 21.9	191.5 ± 27.5	179.6 ± 28.5	205.3 ± 26.4	215.6 ± 42.2
At task end/failure, ms	148.1 ± 27.4	135.0 ± 19.9	141.7 ± 19.8	125.9 ± 15.7	162.8 ± 21.3	168.0 ± 24.1
Central fatigue						
Pre-exercise VA, %	92.4 ± 0.5	93.6 ± 0.7	91.3 ± 0.9	91.5 ± 1.0	92.0 ± 1.3	92.4 ± 1.1
VA at task end/failure, %	91.2 ± 1.6‡	88.0 ± 1.3†	75.0 ± 3.2†	76.1 ± 1.1†	80.0 ± 1.7†	76.9 ± 3.7†
% Change at task end/failure	0.7 ± 0.7	6.0 ± 1.1	17.7 ± 3.6	16.7 ± 1.8	13.0 ± 1.5	16.7 ± 3.8
ΔVA/Δt, %/min	–0.04 ± 0.04‡	–0.2 ± 0.04	–0.9 ± 0.2	–2.1 ± 0.3‡	–2.7 ± 0.4‡	–5.3 ± 1.0‡
Surface EMG						
arEMG at task beginning, % MVC	13.8 ± 1.1	22.2 ± 2.3	35.2 ± 3.1	44.9 ± 4.9	53.7 ± 4.9	61.7 ± 4.3
arEMG at task end/failure, % MVC	14.9 ± 1.3	29.4 ± 4.4	62.4 ± 7.1†	70.1 ± 8.4†	76.5 ± 8.2†	77.6 ± 7.0†
ΔarEMG/Δt, % MVC/min	0.04 ± 0.02‡	0.2 ± 0.1‡	1.6 ± 0.4	3.5 ± 0.9	4.9 ± 1.5	5.4 ± 1.7

Values are means ± SEM. EMG, electromyogram; 50%CT and 90%CT, 50 and 90% of the critical torque, respectively; MVC, maximal voluntary contraction; Δ, change; t, time; VA, voluntary activation; arEMG, average rectified EMG of the vastus lateralis; [a] Mean test torque is expressed as a percentage of the peak torque measured during the MVCs in visit 2. Letters indicate a statistically significant difference compared to the following: *mean test torque, †pre-exercise value/value at task beginning, ‡Severe 1.

Table 2. Variability, complexity and fractal scaling responses to contractions below (50%CTand 90%CT) and above (S1-S4) the critical torque.

Parameter	50%CT	90%CT	S1	S2	S3	S4
SD						
SD at task beginning, N.m	0.9 ± 0.1	1.3 ± 0.1	2.0 ± 0.1	2.4 ± 0.2	2.8 ± 0.3	3.2 ± 0.3
SD at task end/failure, N.m	1.1 ± 0.2†	1.7 ± 0.2†	7.6 ± 0.4*	8.4 ± 0.8*	8.5 ± 1.4*	7.1 ± 0.8*
ΔSD/Δt, N.m.min^{-1} [a]	0.007 ± 0.003†	0.01 ± 0.003†	0.3 ± 0.03	0.8 ± 0.1	1.4 ± 0.4	1.6 ± 0.4
CV						
CV at task beginning, %	3.2 ± 0.2	2.5 ± 0.2	3.0 ± 0.1	3.0 ± 0.2	3.0 ± 0.3	3.0 ± 0.3
CV at task end/failure, %	4.3 ± 0.4†	3.0 ± 0.2†	11.0 ± 1.0*	11.0 ± 1.0*	9.0 ± 1.0*	7.0 ± 0.1*
ΔCV/Δt, %.min^{-1}	0.03 ± 0.01†	0.02 ± 0.01†	0.5 ± 0.04	1.0 ± 0.2	2.0 ± 0.4	2.0 ± 0.5
Force accuracy (RMS error)						
RMS error at task beginning, N.m	2.8 ± 0.6	2.5 ± 0.3	2.7 ± 0.24	3.2 ± 0.3	4.4 ± 0.4	3.9 ± 0.4
RMS error at task end/failure, N.m	2.7 ± 0.5†	3.0 ± 0.5†	9.4 ± 0.5*	11.2 ± 1.2*	11.9 ± 1.7*	11.0 ± 0.9*
ΔRMS error/Δt, N.m.min^{-1} [a]	–0.003 ± 0.01†	0.01 ± 0.01†	0.4 ± 0.02	0.5 ± 0.1	1.4 ± 0.3	2.6 ± 0.3†
ApEn						
ApEn at task beginning	0.93 ± 0.07	0.82 ± 0.03	0.67 ± 0.06	0.52 ± 0.05	0.49 ± 0.05	0.49 ± 0.05
ApEn at task end/failure	0.80 ± 0.07†	0.75 ± 0.06†	0.14 ± 0.01*	0.13 ± 0.02*	0.15 ± 0.04*	0.20 ± 0.03*
ΔApEn/Δt [a]	–0.004 ± 0.002†	–0.002 ± 0.002†	–0.03 ± 0.01	–0.05 ± 0.01	–0.07 ± 0.01†	–0.11 ± 0.01†
DFA α						
DFA α at task beginning	1.31 ± 0.02	1.36 ± 0.01	1.38 ± 0.03	1.42 ± 0.03	1.43 ± 0.03	1.45 ± 0.03
DFA α at task end/failure	1.34 ± 0.03†	1.32 ± 0.03†	1.58 ± 0.01*	1.59 ± 0.02*	1.59 ± 0.02*	1.57 ± 0.03*
ΔDFA α /Δt [a]	0.001 ± 0.001†	–0.001 ± 0.001†	0.01 ± 0.002	0.02 ± 0.005	0.04 ± 0.01†	0.05 ± 0.01†

Values are means ± SEM. 50%CT and 90%CT, 50 and 90% of the critical torque, respectively; Δ, change; t, time; SD, standard deviation; CV, coefficient of variation; RMS error, root mean squared error vs. the target torque; ApEn, approximate entropy; DFA α, detrended fluctuation analysis. Letters indicate a statistically significant difference compared to the following: *pre-exercise value/value at task beginning, †Severe 1. [a]Due to the duration of some trials, discrimination between conditions at 2 decimal places is not possible. Therefore these data are expressed to 2 decimal places or the first significant figure as required.

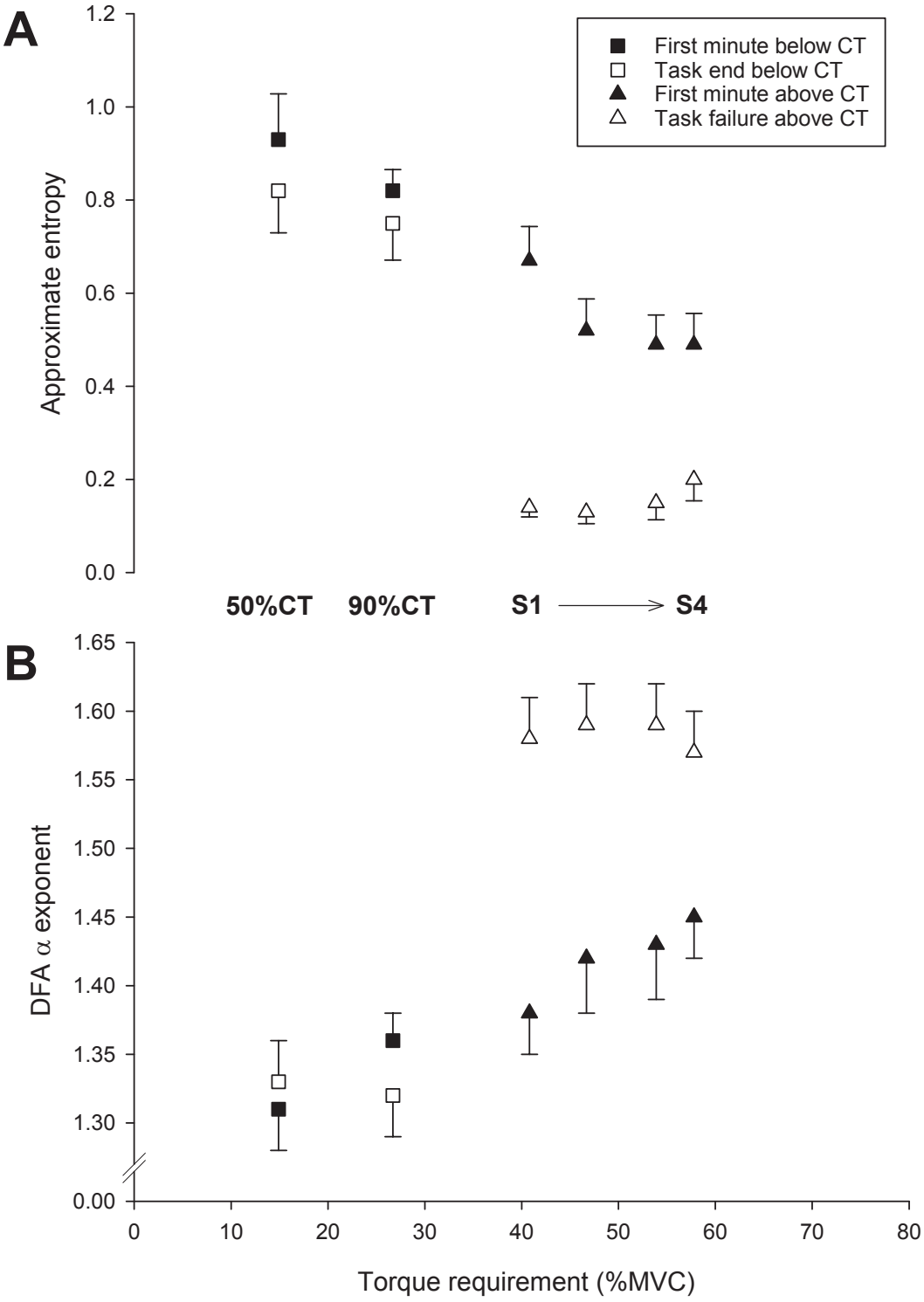
A
Approximate entropy
1.2
1.0
0.8
0.6
0.4
0.2
0.0
First minute below CT
Task end below CT
First minute above CT
Task failure above CT
50%CT
90%CT
S1
S4
B
DFA α exponent
1.65
1.60
1.55
1.50
1.45
1.40
1.35
1.30
0.00
0
10
20
30
40
50
60
70
80
Torque requirement (%MVC)

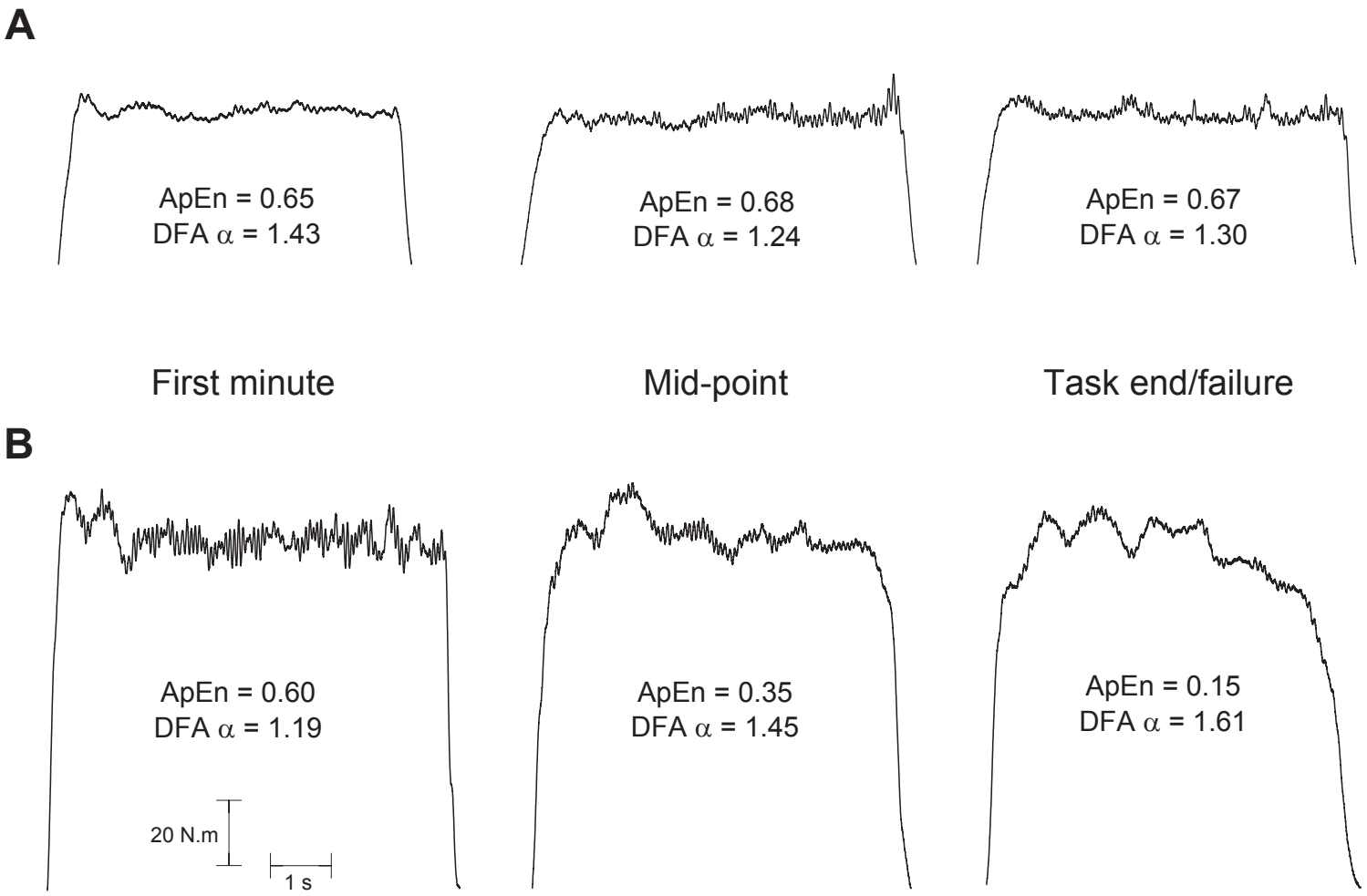
A
ApEn = 0.65
DFA α = 1.43
ApEn = 0.68
DFA α = 1.24
ApEn = 0.67
DFA α = 1.30
First minute
Mid-point
Task end/failure
B
ApEn = 0.60
DFA α = 1.19
20 N.m
1 s
ApEn = 0.35
DFA α = 1.45
ApEn = 0.15
DFA α = 1.61

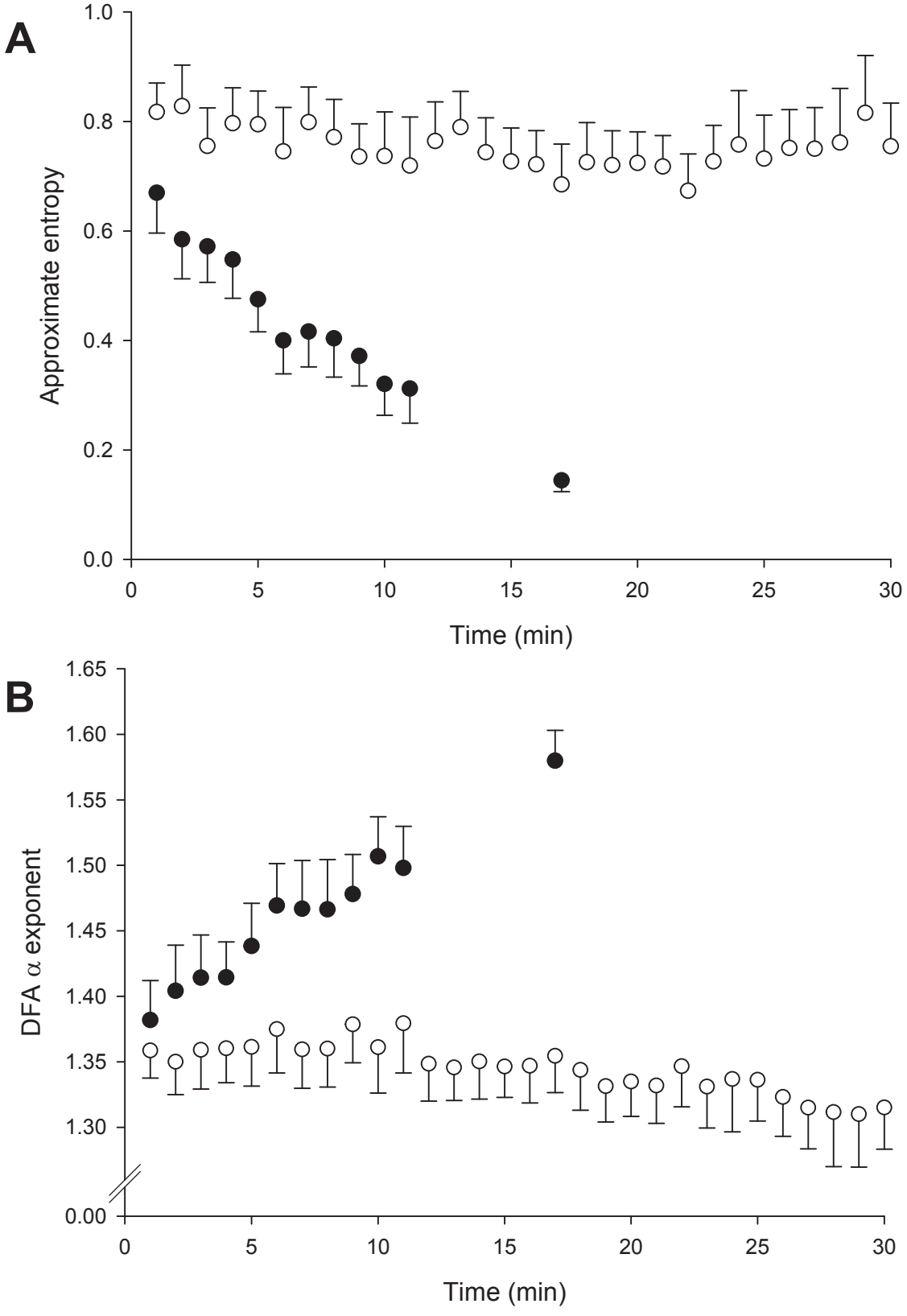
A
Approximate entropy
1.0
0.8
0.6
0.4
0.2
0.0
0
5
10
15
20
25
30
Time (min)
B
DFA α exponent
1.65
1.60
1.55
1.50
1.45
1.40
1.35
1.30
0.00
0
5
10
15
20
25
30
Time (min)

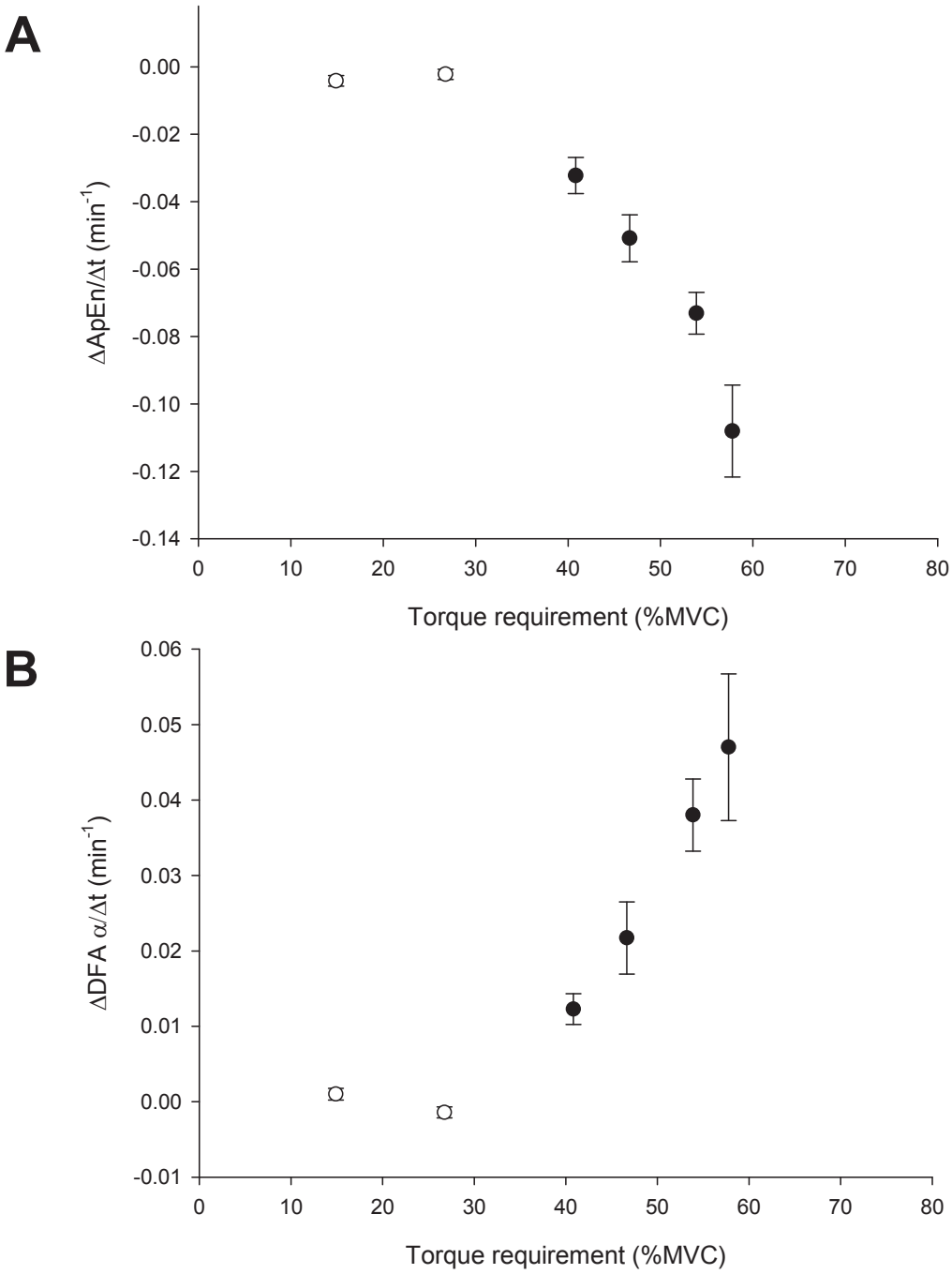
A
0.00
-0.02
-0.04
-0.06
-0.08
-0.10
-0.12
-0.14
ΔApEn/Δt (min-1)
0
10
20
30
40
50
60
70
80
Torque requirement (%MVC)
B
0.06
0.05
0.04
0.03
0.02
0.01
0.00
-0.01
ΔDFA α/Δt (min-1)
0
10
20
30
40
50
60
70
80
Torque requirement (%MVC)